ORIGINAL RESEARCH

Postinfarction Hearts Are Protected by Premature Senescent Cardiomyocytes Via GATA4-Dependent CCN1 Secretion

Sumei Cui, MD;* Li Xue, MD, PhD;* Feihong Yang, MD; Shuai Dai, MD; Ziqi Han, MD; Kai Liu, MD, PhD; Baoshan Liu, MD; Qiuhuan Yuan, PhD; Zhaoqiang Cui, MD, PhD; Yun Zhang, MD, PhD; Feng Xu, MD, PhD; Yuguo Chen, MD, PhD

***Background*—**Stress-induced cell premature senescence participates in a variety of tissue and organ remodeling by secreting such proteins as proinflammatory cytokines, chemokines, and growth factors. However, the role of cardiomyocyte senescence in heart remodeling after acute myocardial infarction has not been thoroughly elucidated to date. Therefore, we sought to clarify the impact of premature myocardial senescence on postinfarction heart function.

***Methods and Results*—**Senescence markers, including $p16^{INK4a}$, $p21^{CIP1/WAF1}$, and SA-β-gal staining, were analyzed in several heart disease models by immunostaining. Both postinfarction mouse hearts and ischemic human myocardium demonstrated increased senescence markers. Additionally, senescence-related secretory phenotype was activated after acute myocardial infarction, which upregulated senescence-related secretory phenotype factors, including CCN family member 1 (CCN1), interleukin-1α, tumor necrosis factor α, and monocyte chemoattractant protein-1. In vivo, a tail vein injection of AAV9-*Gata4*-shRNA significantly attenuated senescence-related secretory phenotype secretion and aggravated postinfarction heart dysfunction. Furthermore, among activated senescence-related secretory phenotype factors, CCN1 administration reduced myofibroblast viability in vitro and rescued the deleterious effect of AAV9-*Gata4*-shRNA in vivo.

***Conclusions*—**Myocardial premature senescence was observed in the ischemic hearts and improved postinfarction heart function, partly through the GATA-binding factor 4-CCN1 pathway. **(*J Am Heart Assoc*. 2018;7:e009111. DOI: 10.1161/JAHA.118.009111.)**

Key Words: CCN1 • fibrosis • myocardial ischemia • senescence

Despite advances in the treatment of acute myocardial infarction (AMI), many patients still develop progressive heart failure in several years as a result of declining cardiac function.[1–4] This situation suggests that there are missing pathophysiological mechanisms, which motivates researchers to explore viable strategies to preserve post-AMI cardiac function.

Cellular senescence was traditionally defined as the state of irreversible cell cycle arrest after cells reached a maximal number of divisions; this process is termed "replicative senescence."[5] Functionally, it was believed that senescence caused senescence-related functional decline. However, these concepts have been redefined by recent studies. Stress-induced senescence or age-independent premature senescence is used to describe the phenomenon in which various stressors, such as oncogenic events and ionizing radiation, instigate cellular dysfunction.[6,7] Additionally, it is becoming evident that senescence also exerts beneficial roles in normal embryonic development and tissue repair processes.[8–10] Mechanically, senescent cells can affect surrounding cells and play active roles in tissue remodeling by secreting such

From the Department of Emergency (S.C., L.X., F.Y., S.D., Z.H., B.L., Q.Y., F.X., Y.C.), Chest Pain Center (S.C., L.X., F.Y., S.D., Z.H., B.L., Q.Y., F.X., Y.C.), Key Laboratory of Emergency and Critical Care Medicine of Shandong Province (S.C., L.X., F.Y., S.D., Z.H., B.L., Q.Y., F.X., Y.C.), Key Laboratory of Cardiovascular Remodeling & Function Research, Chinese Ministry of Education & Chinese Ministry of Public Health (S.C., L.X., F.Y., S.D., Z.H., B.L., Q.Y., Y.Z., F.X., Y.C.), and Cardiovascular Surgery Department (K.L.), Qilu Hospital, and Institute of Emergency and Critical Care Medicine (S.C., L.X., F.Y., S.D., Z.H., B.L., Q.Y., F.X., Y.C.), Shandong University, Jinan, China; Shanghai Institute of Cardiovascular Diseases, Zhongshan Hospital, Fudan University, Shanghai, China (Z.C.).

Accompanying Table S1 and Figures S1 through S5 are available at https://www.ahajournals.org/doi/suppl/10.1161/JAHA.118.009111

*Dr Sumei Cui and Dr Xue contributed equally to this work.

Correspondence to: Feng Xu, MD, PhD and Yuguo Chen, MD, PhD, Department of Emergency, Shandong University Qilu Hospital, 107 Wenhuaxi Rd, Jinan 250012, China. E-mails: xufengsdu@126.com; chen919085@sdu.edu.cn

Received March 21, 2018; accepted July 31, 2018.

© 2018 The Authors. Published on behalf of the American Heart Association, Inc., by Wiley. This is an open access article under the terms of the Creative Commons Attribution-NonCommercial License, which permits use, distribution and reproduction in any medium, provided the original work is properly cited and is not used for commercial purposes.

Clinical Perspective

What Is New?

- Senescence phenotype was activated in multiple rodent heart diseases including post–acute myocardial infarction mouse myocardium, isoproterenol-treated mouse hearts, and human ischemic heart tissues.
- Myocardial senescence was necessary to prevent the post–acute myocardial infarction pathological fibrosis and heart dysfunction through the GATA-binding factor 4-CCN1 pathway.
- Aldehyde dehydrogenase2 knockout impaired the beneficial effects of myocardial senescence by blocking the GATA-binding factor 4-CCN1 pathway.

What Are the Clinical Perspectives?

- Understanding the precise mechanism behind myocardial senescence helps in the development of new drugs and in determining appropriate clinical strategies in the future.
- Regulating the GATA-binding factor 4-related pathway is promising for improving cardiac remodeling in aldehyde dehydrogenase2 mutant-type persons.

proteins as proinflammatory cytokines, chemokines, and growth factors (senescence-associated secretory phenotype, SASP).[11] GATA-binding factor 4 (GATA4) is required to maintain senescence and SASP.[12] Upon DNA damage response, GATA4 is activated and in turn, initiates the secretion of inflammation factors by activating transcription factor NF-kB.[12] Furthermore, it was verified that GATA4-mediated senescence and secretory phenotype are involved in multiple aging tissues including brain, skin, and liver.[12] In this study, we investigated whether cardiomyocyte senescence participated in post-AMI heart remodeling and whether the underlying mechanism is related to GATA4.

CCN family member 1 (CCN1, also known as CYR61) is an important component of SASP and can restrict pathological fibrosis in liver and wound healing.[13,14] In the heart, ischemia/reperfusion induces CCN1 expression in cardiomyocytes, serving as an autocrine function to mediate the cardioprotective effects.[15] Another study demonstrated that cardiac-specific overexpression of CCN1 possessed antifibrosis effects in cardiac fibrosis, suggesting that CCN1 linked a cardiomyocyte–fibroblast interaction.[10] Considering that pathological fibrosis is vital in AMI-induced heart malfunction, we speculate that cardiomyocyte-derived CCN1 may protect the heart by preventing pathological fibrosis.

It was reported that myofibroblast senescence possessed antifibrosis effects in cardiac fibrosis.[10] Moreover, cardiomyocyte senescence is implicated in the myocardial damage caused by doxorubicin and obesity.[16,17] However, as the primary cell population that constitutes ≈75% of the myocardium volume,[18] the contribution of cardiomyocyte senescence to heart remodeling has not been thoroughly elucidated to date. Thus, we examined the implication of cardiomyocyte senescence in post-AMI cardiac tissues and the contribution to post-AMI cardiac function, as well as its mechanisms in this study.

Materials and Methods

The authors declare that all supporting data are available within the article and its online supplementary files.

Human Heart Samples

Human left ventricular (LV) samples, which were from deceased donors in Shandong University Qilu Hospital, were separated into ischemic and control groups based on whether coronary atherosclerotic plaques were observed during the autopsy.

Senescence-associated-ß-galactosidase (SA-ß-gal) staining was performed on human right atrium samples, while samples from 6 patients who underwent coronary artery bypass graft surgery were included as the ischemic group, and age-matched patients undergoing mitral valve replacement surgery were included as the controls. Written consent was obtained before surgery or donation. The study complied with the Declaration of Helsinki and was approved by the Institutional Ethics Committee at the institution.

Mouse AMI Models

Aldehyde dehydrogenase2 (ALDH2) knockout mice (KO) were purchased from Riken Bioresource Center (Ibaraki, Japan) and backcrossed with wild-type C57BL/6 mice from the Department of Experimental Animals of Shandong University (Jinan, China) for 1 year. The mice were kept at a constant temperature with a 12-hour light/dark cycle and free access to standard diet and water. Eight- to 12-week-old male littermate mice were used in the study and randomization was performed. Experimental AMI was produced by ligation of the left anterior descending coronary artery as described previously.[19] All animal experimental procedures were performed under the Guide for the Care and Use of Laboratory Animals and were approved by the Institutional Animal Care and Use Committee of Shandong University.[20]

Diabetes Mellitus and Heart Failure Models

Adult male Wistar rats (200–250 g) were purchased from the Department of Experimental Animals of Shandong University (Jinan, China). The rats were kept at a constant temperature with a 12-hour light/dark cycle and free access to standard diet and water. Streptozocin-induced diabetic

rats were generated using the method published by our group.[21] The heart failure model was generated by subcutaneous isoproterenol injection once daily for 3 consecutive days (100 mg/kg), while isotonic saline-injected rats served as the control group.

Antibodies and Reagents

The following primary antibodies were used: anti-p53 (Abcam, UK), anti-$p16^{INK4a}$ (Abcam, UK), anti-$p16^{INK4a}$ (Abcam, UK), anti-$p21^{CIP1/WAF1}$ (Abcam, UK), anti-GATA4 (Santa-Cruz, USA), anti-GATA4 (Abcam, UK), anti-CCN1 (Abcam, UK), anti-γ-H2AX (Abcam, UK), anti-γ-H2AX (CST, USA), anti-GAPDH (Proteintech, China), anti-β-actin (Boster, China), anti-interleukin (IL)-1α (Proteintech, China), anti–monocyte chemotactic protein-1 (Abcam, UK), anti–tumor necrosis factor-α (TNF-α) (Abcam, UK), and anti-α-actin (Proteintech, China). All secondary antibodies were from ZSGB-BIO Company (China). Reagents wheat germ agglutinin and Alda-1 were purchased from Sigma-Aldrich, USA. All of the catalog numbers of the antibodies are listed in Table S1.

Cell Culture

Neonatal rat cardiac myocytes and fibroblasts were isolated as previously reported.[22] The senescent cardiomyocyte model was established by culturing neonatal rat cardiac myocytes under hypoxia (1% O_2, 5% CO_2, 94% N_2) for 10 hours, manifesting as significantly increased SA-β-gal activity. Small interfering RNAs against GATA4 were purchased from GenePharma (Shanghai, China) and transduced into neonatal rat cardiac myocytes with Lipofectamine 3000 (Thermo Fisher, USA). The Gata4-small interfering RNAs sequence was 5′-GGCCUCUAUCACAAGAUGA-3′.

Transfection of Adeno-Associated Virus

Adeno-associated virus subtype 9 containing *Gata4*-shRNA (AAV9-*Gata4*-shRNA) and negative-control vectors (AAV9-NC) were purchased from Genepharma (Shanghai, China). The *Gata4*-shRNA sequence was GGCCTCTATCACAAGATGA. The virus (8.0×10^{11} V.G/mouse) was injected via the tail vein 4 weeks before AMI surgery.

SA-β-gal Staining

In vitro, senescence β-Galactosidase Staining Kit (CST, #9860) was utilized according to the instruction manual. Fresh heart tissues were washed in PBS 3 times and incubated in artificial SA-β-gal staining solution overnight at 37°C. After that step, the hearts were placed in OCT compound (SAKURA, 4583) and cut into 10-μm sections to take pictures with bright-field microscopy (Olympics, IX73+DP73).

CCN1 Administration and Cell Viability Assay

Recombinant human CCN1 protein was purchased from Proteintech, China. In vitro recombinant CCN1 protein diluted in DMEM medium was used, while BSA served as the control. The cell viability assay was performed with Cell Counting Kit-8 (MCE, USA) according to the manufacturer's instructions. CCN1 protein was diluted in saline solution and administered by daily tail vein injection from 2 weeks postinfarction to 4 weeks postinfarction.

Western Blotting

Tissue or cell lysates with the same protein content (assayed by the BCA method; Bio-Rad, CA) were prepared. Proteins were separated by 10% SDS-PAGE or 12% SDS-PAGE and transferred to a polyvinylidene difluoride membrane (Millipore). The membranes were blocked for 1.5 hours in 3% milk and then incubated overnight at 4°C with primary antibodies, followed by horseradish peroxidase–conjugated rabbit anti-goat (1:5000) or goat anti-rabbit immunoglobulin G (1:5000 or 1:10 000) for 2 hours at room temperature. The bands were scanned and detected by a standard enhanced chemiluminescence method with Chemiluminescent HRP Substrate (Millipore, WBKLS0100). ImageJ Software was used to quantitate the intensity of the bands.

Histochemical Staining and Analysis

The mice were euthanized at designated time points after the AMI procedure. The hearts were fixed with 10% formalin for 24 hours at room temperature before being embedded in paraffin for sectioning. Tissues were sectioned at 5 mm and underwent immunohistochemical staining as standard protocols. Images were captured using a microscope (Olympus, X41) and were analyzed by using Image-Pro Plus 6.0. Masson staining was performed in 3 sections and utilized to assess the fibrosis.

Echocardiography

An ultrasound machine (Vevo2100 imaging system) was used to assess mouse left ventricular diameter and function by the M-mode images of the parasternal long- and short-axis views. During the whole process, mice were anesthetized with isoflurane, and the heart rates were maintained at more than 450 beats per minute.

Measurement of Cardiac Troponin T

After 24 hours of infarction surgery, the cardiac Troponin T in the serum was detected with the ELISA kit (Cloud Clone, SEB820Mu) following the instructions.

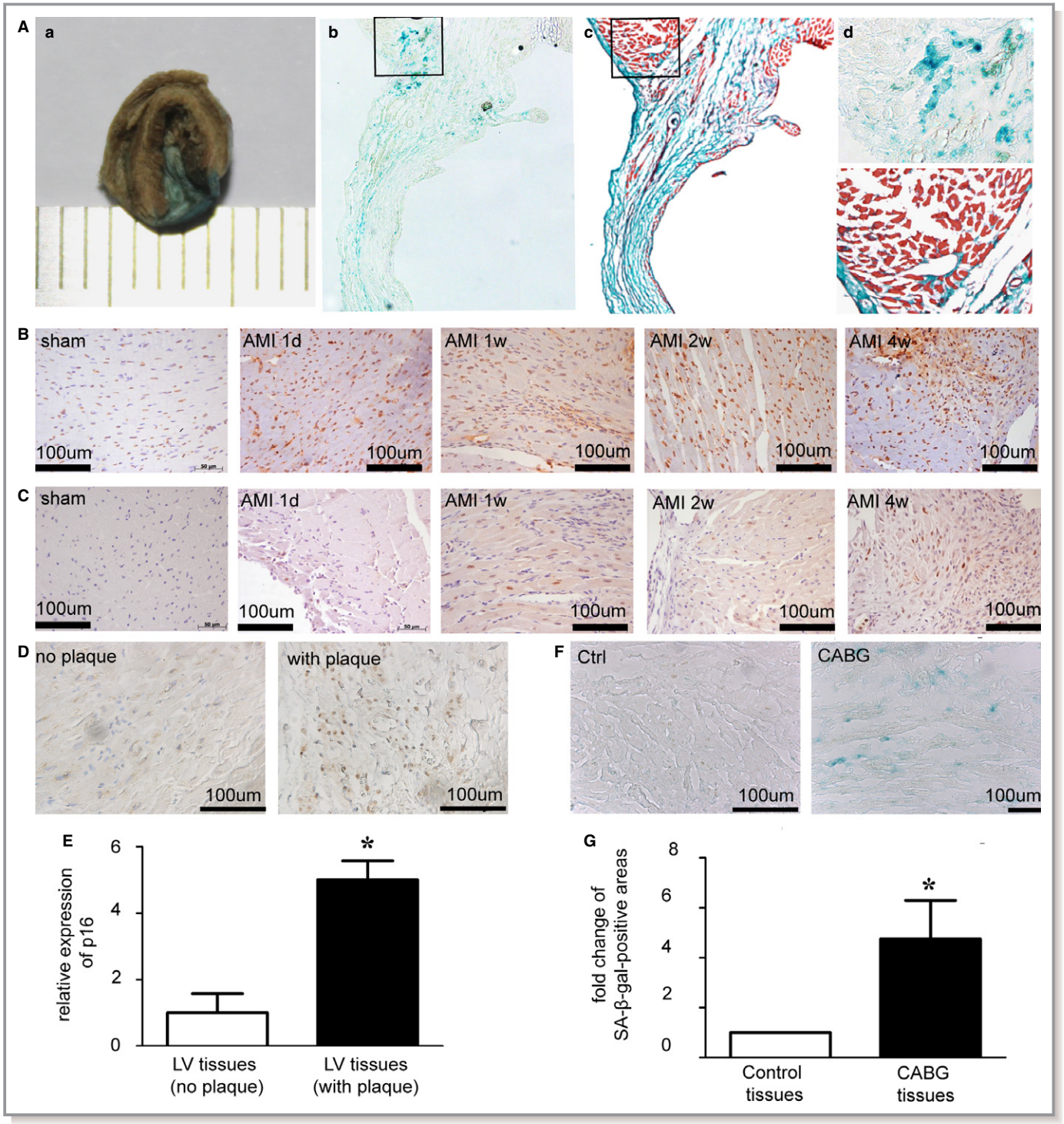

Figure 1. Senescence biomarkers accumulated in ischemic hearts. A, Gross senescence-associated-β-galactosidase (SA-β-gal) staining pictures in the heart (a) and SA-β-gal staining pictures in the heart sections (b and d), as well as Masson staining pictures (c and e) on day 28 post–acute myocardial infarction (AMI). B, Representative immunohistochemical pictures of $p16^{INK4a}$ in the border zones at first d, first wk, second wk, and fourth wk after AMI. C, Representative immunohistochemical pictures of $p21^{CIP1/WAF1}$ in the border zones at first d, first wk, second wks, and fourth week after AMI. D, Representative immunohistochemical pictures of $p16^{INK4a}$ in human left ventricular (LV) tissues with and without coronary plaques. E, Fold change of $p16^{INK4a}$ expression between human LV tissues with and without coronary plaques. ImageJ was used for immunohistochemical analysis. *P<0.05 vs LV tissues without plaques (n=4 for the control group and n=6 for the group with plaques). F, SA-β-gal staining in the right auricle from patients undergoing mitral valve replacement surgeries (as the control group) and coronary artery bypass graft (CABG) surgeries. G, Fold change of the SA-β-gal-positive cells between control and CABG right auricles. *P<0.05 vs control tissues (n=3 for control group and n=6 for CABG group).

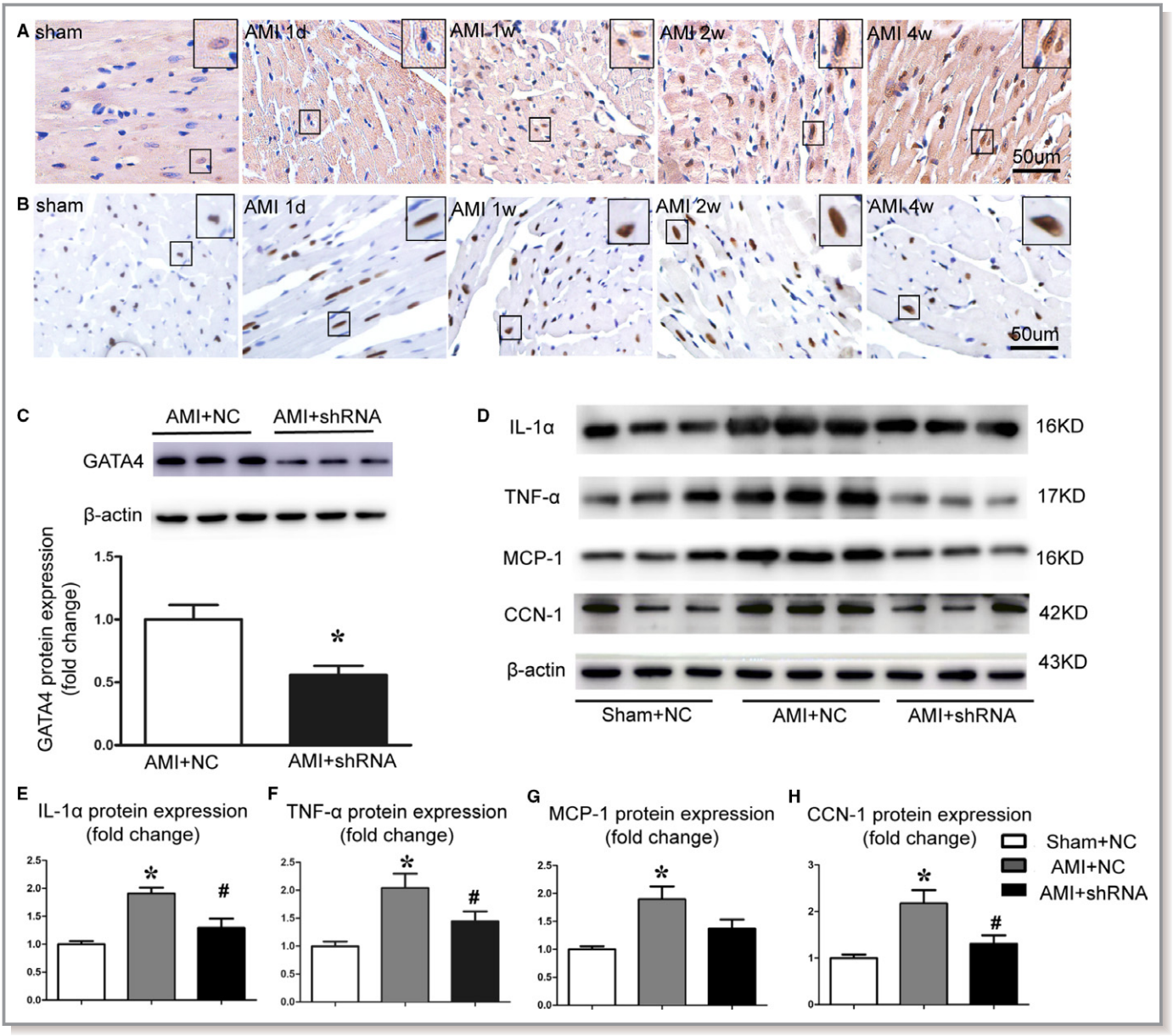

Figure 2. GATA4 knockdown suppressed the activation of senescence-related secretory phenotype (SASP) after AMI. A, Representative immunohistochemical pictures of γ-H2AX confirmed the DNA damage response in border areas. B, Representative immunohistochemical pictures of GATA4 in post-AMI border areas. C, Efficacy of GATA4 knockdown by AAV9-*Gata4*-shRNA compared with negative control vectors (NC); **P*<0.05 vs NC group (n=3). D, Western blotting was performed to examine the change of selected SASP factors including IL-1α, MCP-1, TNF-α, and CCN1 in the post-AMI border tissues. E through H, Quantitation and fold changes of IL-1α, MCP-1, TNF-α, and CCN1 after AMI. **P*<0.05 vs sham mice with negative control AAV9 vector (NC); #*P*<0.05 vs AMI mice with negative control AAV9 vector (NC) (n=6). AMI indicates acute myocardial infarction; CCN1, CCN family member 1; GATA4, GATA-binding factor 4; MCP-1, monocyte chemotactic protein-1; TNF-α, tumor necrosis factor-α.

Statistical Analysis

Results are reported as the mean±SEM. After checking the assumptions of normality, statistical significance was accomplished using an ANOVA test and unpaired Student *t* test unless specifically stated. *P*<0.05 is considered to be statistically significant.

Results

Senescence Biomarkers Accumulated in Ischemic Hearts

SA-ß-gal staining permits the identification of senescent cells in postinfarction tissues. As Figure 1A demonstrates,

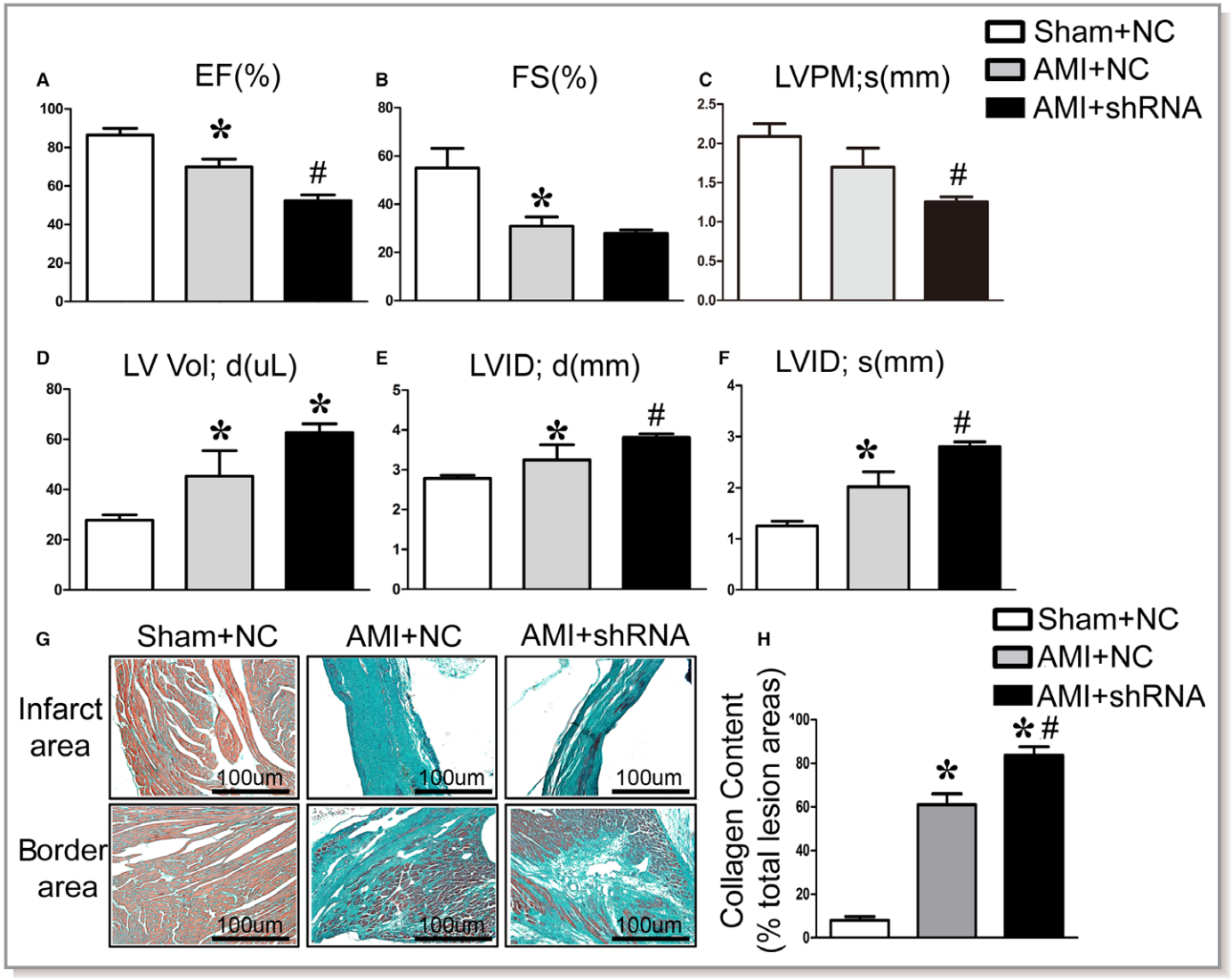

Figure 3. GATA4 was essential to preserve post-AMI heart function. A through F, Echocardiography was used to measure heart function among the Sham+NC, AMI+NC, AMI+Gata4-shRNA groups. The following parameters were assessed: left ventricular ejection fraction (LVEF), fractional shortening (FS), LV posterior wall at end-systolic (LVPM; s), left ventricular end-systolic (LVID; s), end-diastolic internal diameter (LVID; d) and LV end-diastolic volume (LV Vol; d). **P*<0.05 vs sham+NC group; #*P*<0.05 vs AMI+NC group; n=6. G, Representative Masson staining pictures. H, ImageJ was utilized to evaluate fibrosis that was quantitated as the ratio of the green area to the total LV free wall. **P*<0.05 vs sham. **P*<0.05 vs sham; #*P*<0.05 vs AMI (n=6). AMI indicates acute myocardial infarction; EF, ejection fraction; GATA4, GATA-binding factor 4; NC, negative control vectors.

SA-ß-gal-positive senescent cells accumulated both in the infarct and border areas 4 weeks after AMI surgeries. Masson staining showed that the SA-ß-gal-positive senescent cells seemed colocalized with the cardiomyocytes in the border areas (Figure 1A). This conclusion was further confirmed by the observation that α-actin-positive cardiomyocytes showed increased senescence marker $p16^{Ink4a}$ in the border zones (Figure S1A). In our previous study, we utilized Western blotting to observe a time-dependent increase of senescence biomarkers, including p53 and $p16^{Ink4a}$ in postinfarction myocardium.[23] Histological analysis confirmed that senescence marker $p16^{INK4a}$ increased as early as 1 day and lasted for 4 weeks after left anterior descending coronary artery ligation (Figure 1B). Additionally, another senescence marker $p21^{CIP1/WAF1}$ was upregulated, beginning at 1-week postinfarction and lasting for 4 weeks after left anterior descending coronary artery surgery (Figure 1C).

Of interest, senescence phenotype was activated in human ischemic heart tissues. Compared with human LV without coronary plaques, $p16^{INK4a}$ increased ≈5-fold in LV tissues with coronary plaques (Figure 1D and 1E). Additionally, the number of SA-ß-gal-positive cells increased ≈4-fold in heart tissues from coronary artery bypass graft patients compared with those from the control group (Figure 1F and 1G, Figure S1B). Furthermore, the α-actin-positive cardiomyocytes displayed upregulated senescence marker $p16^{INK4a}$ in the heart

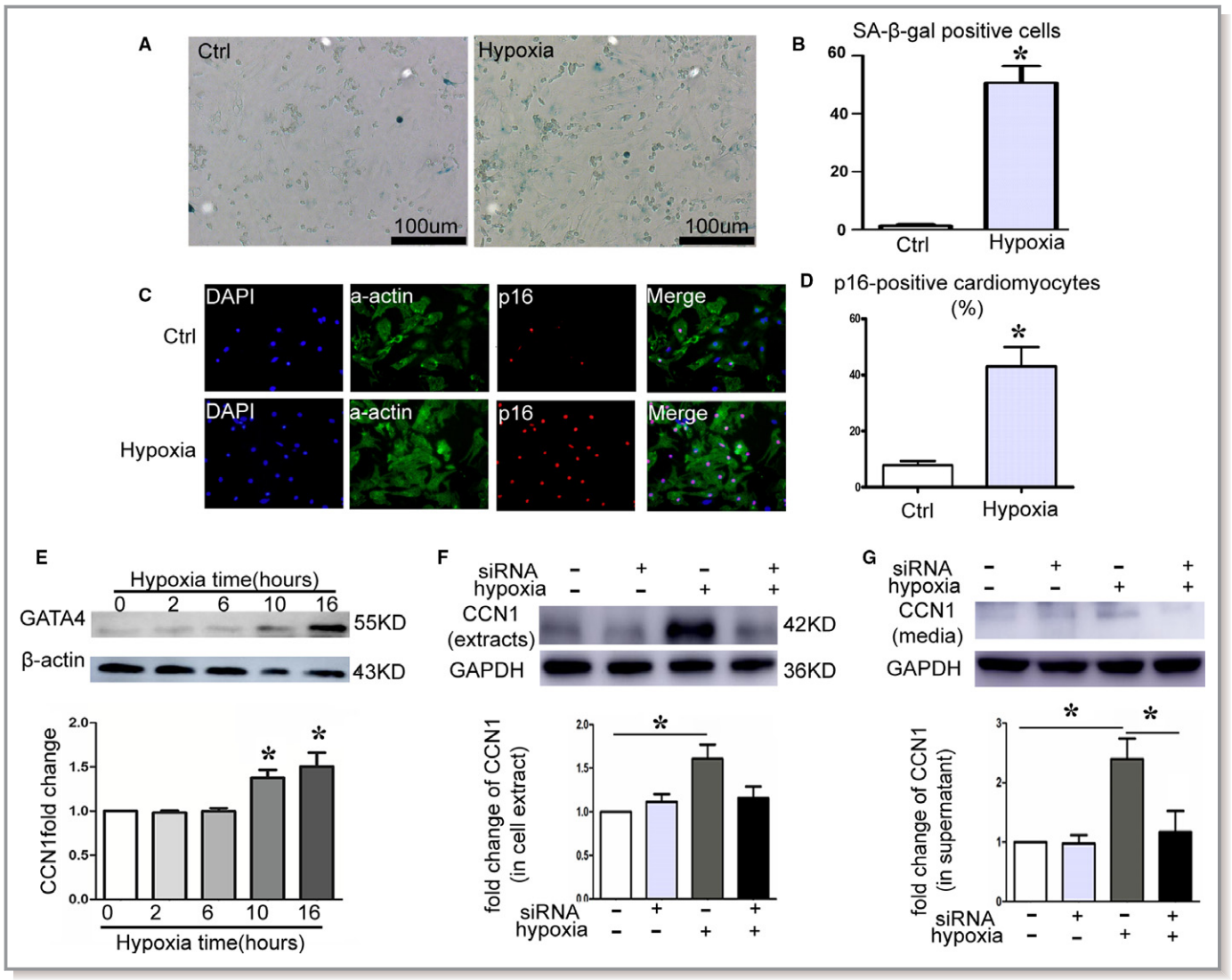

Figure 4. Generation of senescent cell models. A, SA-β-gal staining images in the neonatal rat cardiac myocytes (NRCMs) after being cultured in hypoxia for 10 h. B, Quantitative analysis of SA-β-gal-positive NRCMs. **P*<0.05 vs control (n=6 for control group and n=8 for the hypoxia group). C, Immunofluorescence staining images for DAPI (blue), α-actin (green), and $p16^{INK4a}$ (red) in the NRCMs after hypoxia. D, Quantitative analysis of $p16^{INK4a}$-positive cardiomyocytes. **P*<0.05 vs control (n=4). E, Western blotting was performed to show a time-dependent GATA4 protein accumulation after being cultured at hypoxia for different hours and repeated measures analysis was used to analyze the statistics. **P*<0.05 vs 0 hour (n=3). F, *Gata4*-siRNA downregulated the hypoxia-induced-CCN1 increase in cell extracts by Western blotting and ImageJ was used to analyze the data. **P*<0.05 (n=3). G, *Gata4*-siRNA downregulated the hypoxia-induced-CCN1 increase in cell supernatant by Western blotting and ImageJ was used to analyze the data. **P*<0.05 (n=3). CCN1 indicates CCN family member 1; Ctrl, control; DAPI, 4′,6-diamidino-2-phenylindole; GATA4, GATA-binding factor 4; SA-β-gal, senescence-associated-β-galactosidase.

tissues of coronary artery bypass graft patients (Figure S1C and S1D). In other cardiac injury models, $p16^{INK4a}$ also increased in streptozocin-induced rat hearts (Figure S1E) and the isoproterenol-treated rat hearts (Figure S1F).

GATA4-Dependent SASP Was Activated in Ischemia-Induced Senescent Cardiomyocytes

GATA4 was identified as the key mediator of SASP, which was activated by damaged DNA and able to influence multiple tissue-remodeling in a context-dependent manner.[12] In this study, we observed increased cardiomyocytes with damaged DNA based on γ-H2AX immunostaining in postinfarction hearts (Figure 2A). As the downstream of damaged DNA, GATA4 was raised accordingly in post-AMI myocardium in the border areas (Figure 2B). To examine the effects of GATA4 inhibition on activated SASP, we utilized AAV9-*Gata4*-shRNA to achieve 50% GATA4 knockdown in vivo (Figure 2C, Figure S2A). Western blotting revealed that the SASP was effectively activated after AMI because selected SASP factors

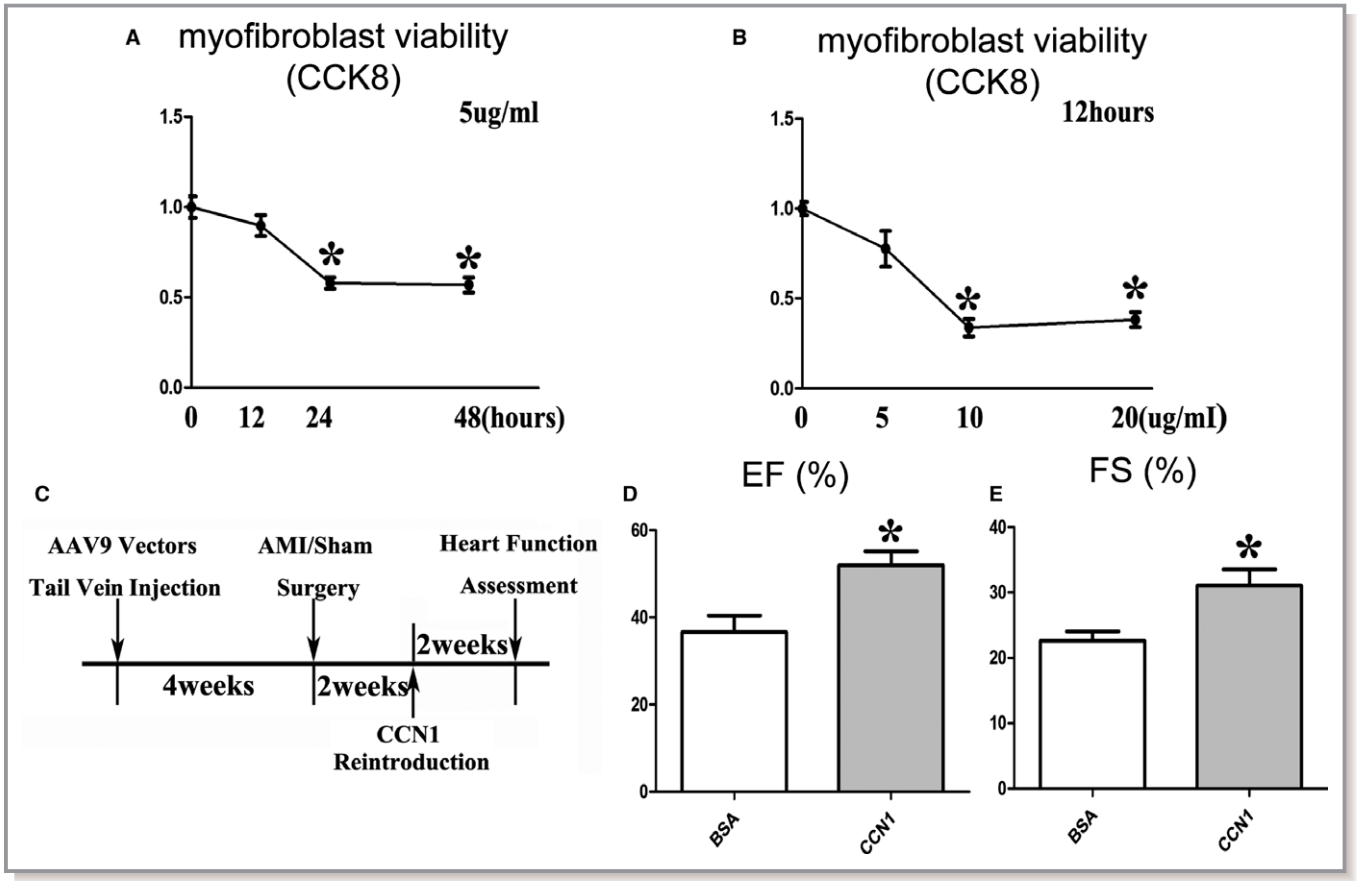

Figure 5. CCN1 administration reduced myofibroblast viability and preserved heart function in *Gata4*-shRNA. A, Time-dependent effects of exogenous CCN1 (5 μg/mL) on myofibroblast viability by the CCK8 assay and repeated measures analysis was used to analyze the statistics. **P*<0.05 vs 0 hour (n=5). B, Dose-dependent effects of CCN1 administration on myofibroblast vitality, detected by CCK8 assay. **P*<0.05 vs 0 μg/mL (n=3). C, Strategy of the CCN1 rescue experiment. D and E, Echocardiography showed that CCN1 rescued the impaired LVEF (D) and FS (E) in *Gata4*-shRNA mice after AMI, while BSA treatment had no effect. **P*<0.05 vs BSA group (n=6 for BSA group and n=7 for CCN1 group). AMI indicates acute myocardial infarction; BSA, bovine serum albumin; CCN1, CCN family member 1; EF, ejection fraction; FS, fractional shortening; LVEF, left ventricular ejection fraction.

including IL-1α, TNF-α, monocyte chemotactic protein-1, and CCN1 were significantly increased after AMI (Figure 2D through 2H). Compared with negative-control vectors (NC), AAV9-*Gata4*-shRNA significantly downregulated activated SASP factors IL-1α, TNF-α, and CCN1 (Figure 2D through 2H). Taken together, these findings indicate that GATA4 accumulates in the damaged DNA after AMI and is required for postinfarction SASP activation.

GATA4 Inhibition Aggravated Postinfarction Heart Dysfunction and Fibrosis

Echocardiography was utilized to assess heart function after mice were transfected with AAV9-*Gata4*-shRNA or negative control vectors. As data demonstrate, the impaired LV ejection fraction and fractional shortening were further deteriorated by AAV9-*Gata4*-shRNA 4 weeks after left anterior descending coronary artery ligation (Figure 3A and 3B), although there is no significance in the cardiac Troponin T levels in serum 24 hours postinfarct induction (Figure S2B). Furthermore, the LV posterior wall at end-systolic (LVPM; s) became thinner after AAV9-Gata4-shRNA administration (Figure 3C). Furthermore, the post-AMI hearts displayed LV dilatation as left ventricular end-systolic (LVID; s), end-diastolic internal diameter (LVID; d), and left ventricular end-diastolic volume (LV Vol; d) were significantly increased. The dilated phenotype was further exaggerated by GATA4 knockdown (Figure 3D through 3F). In addition, the collagen content was upregulated from 60% to 80% of the total lesion areas by Masson staining (Figure 3G and 3H). These data suggested that GATA4 was required for post-AMI heart recovery, and GATA4-mediated SASP exerted protective effects in post-AMI functional restoration.

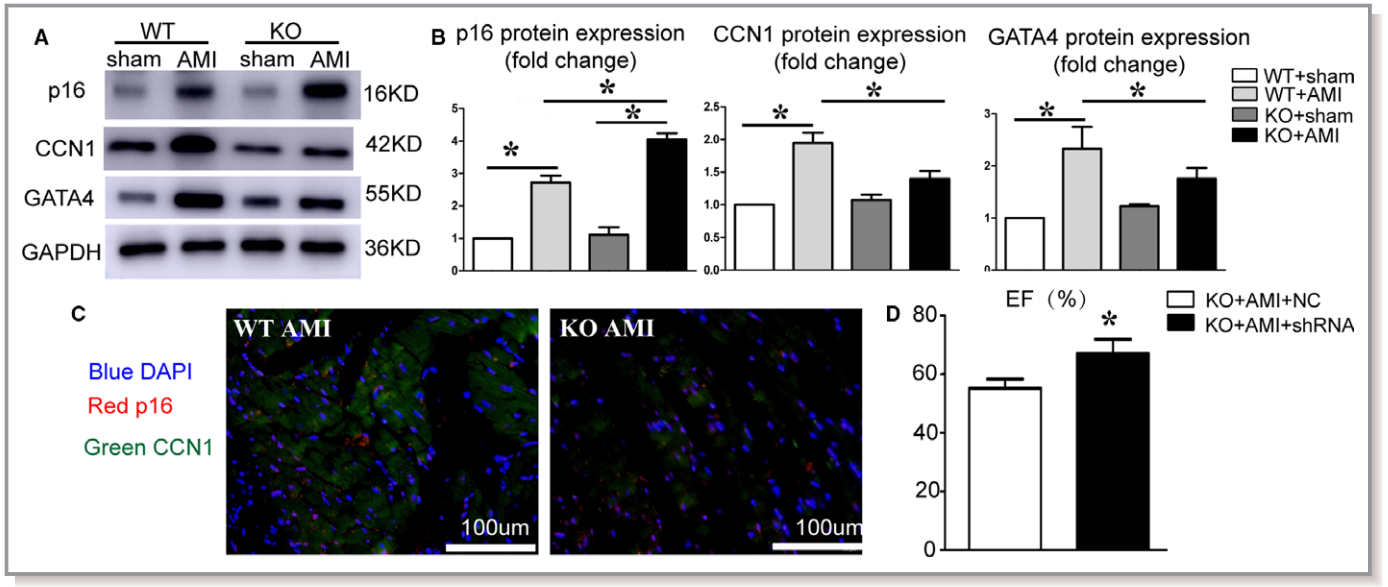

Figure 6. ALDH2 deficiency impaired GATA4-CCN1-fibrosis pathway after AMI. A, Western blotting was utilized to examine the protein change increasing $p16^{INK4a}$, CCN1, and GATA4 after AMI between wild-type (WT) and ALDH2 knockout (KO) mice. B, Quantitative analysis of the Western blotting. *P<0.05 (n=3). C, Compared with WT mice, KO mice showed decreased protein CCN1 expression in $p16^{INK4a}$-positive cells after AMI treatments. Immunofluorescent staining was performed in this experiment. D, Echocardiography showed that Gata4-shRNA improved impaired EF in the $Aldh2^{-/-}$ post-AMI mice. *P<0.05 vs negative control (NC) AAV9 (n=6 for WT group and n=8 for KO mice). ALDH2 indicates aldehyde dehydrogenase2; AMI, acute myocardial infarction; CCN1, CCN family member 1; DAPI, 4′,6-diamidino-2-phenylindole; EF, ejection fraction; GATA4, GATA-binding factor 4; KO, knockout mice; WT, wild-type.

CCN1 Rescued the Deleterious Effect of AAV9-Gata4-shRNA

We isolated and cultured neonatal rat cardiac myocytes to recapitulate postinfarction cardiomyocyte senescence in vitro. The immunofluorescence staining verified >80% of cells as α-actin-positive cardiomyocytes (Figure S3). The senescence cell model was successfully established and was characterized by increased SA-β-gal-positive cells (Figure 4A and 4B). Similarly, the number of p16-positive cardiomyocytes increased after hypoxia (Figure 4C and 4D). Western blotting confirmed a time-dependent GATA4 protein increase in vitro (Figure 4E).

Of note, CCN1 has antifibrosis and cardiac protective potential among the activated SASP factors. Consistent with the in vivo observation that GATA4 was required for SASP activation (Figure 2D and 2H), *Gata4*-small interfering RNAs significantly suppressed CCN1 increases in both cell extracts and supernatants (Figure 4F and 4G). The CCK8 assay demonstrated that exogenous CCN1 protein negatively regulated fibroblast viability in a time-dependent and dose-dependent pattern (Figure 5A and 5B), corroborating previous reports that CCN1 directly downregulates fibroblast viability.[13,14] Next, we re-introduced recombinant CCN1 protein to *Gata4*-shRNA mice by tail vein injection (Figure 5C), which caused more than a 3-fold increase of CCN1 in the heart tissues 24 hours after injection (Figure S4). Compared with the BSA control group, CCN1 administration effectively reserved cardiac function 4 weeks after surgery (Figure 5D and 5E). Taken together, these results suggest that GATA4-related CCN1 secretion participates in the heart function preservation of senescent cardiomyocytes.

ALDH2 Deficiency Blocked GATA4-CCN1 Pathway After AMI

We have a longstanding interest in the effects of ALDH2 and the cardiovascular system.[24–26] We previously found that ALDH2 activation by Alda-1 reduced the senescence phenotype in H9C2 cell lines.[23] Compared with wild-type mice, $Aldh2^{-/-}$ mice manifested increased $p16^{INK4a}$ expression with unaltered GATA4 and CCN1 expression levels after AMI, via Western blotting (Figure 6A and 6B). In addition, immunofluorescence staining indicated a reduction of CCN1 in $p16^{INK4a}$-positive senescent after AMI, compared with wild-type mice (Figure 6C). Functionally, GATA4 inhibition was observed to alleviate the impaired heart function as ejection fraction was statistically restored after AMI (Figure 6D).

Discussion

The present investigation is a continuation and extension of our earlier work that provided primary evidence on the activated senescence-associated phenotype after AMI.[26] In

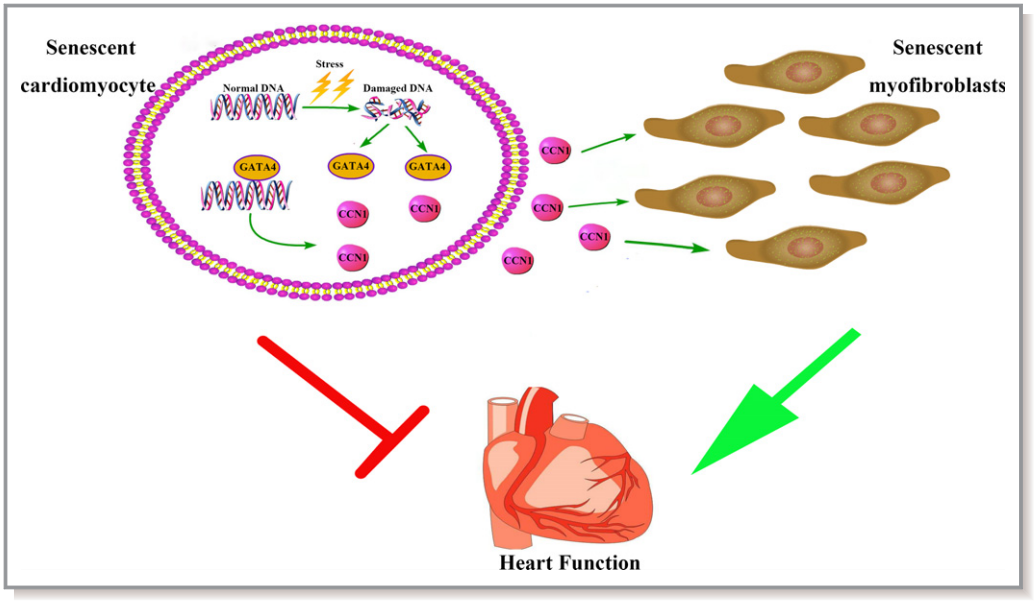

Figure 7. Mechanistic working model describing the role of myocardial senescence in post-AMI heart remodeling. In summary, post-AMI cardiomyocyte senescence involved in heart remodeling via the balance between direct senescence-related dysfunction and antifibrosis effects of GATA4-dependent CCN1 secretion. Red lines indicate negative effects to heart recovery and green lines for protective roles on the heart. AMI indicates acute myocardial infarction; CCN1, CCN family member 1; GATA4, GATA-binding factor 4.

this study, we determined that myocardial senescence is involved in multiple rodent heart diseases and human ischemic heart tissues. We verified that cardiomyocyte senescence was essential to postinfarction heart function via the GATA4-CCN1 pathway to exert antifibrosis effects. This discovery is in keeping with recent findings that pro-senescence therapies can be beneficial to the tissue and organ.[27]

We combined several senescence markers to confirm the activated senescence phenotype in mouse and human disease models, including immunostaining of $p16^{Ink4a}$ and $p21^{CIP1/WAF1}$, as well as SA-β-gal staining. Masson staining and dual immunofluorescence staining were included to establish that cardiomyocytes underwent senescence after hypoxia. Regarding its functional role, SASP was important for senescence to participate in tissue remodeling that was maintained by transcription factor GATA4.[12] In this study, we noticed an increase of GATA4 accumulation in the border zones, where the senescence markers are also highly expressed. Moreover, AAV9-*Gata4*-shRNA sustainably downregulated SASP secretion after AMI, as selected SASP factors IL-1α, monocyte chemotactic protein-1, TNF-α, and CCN1 were all reduced by *GATA4*-shRNA. This observation was consistent with Kang's report, suggesting that GATA4 not only mediates SASP in vitro but also in vivo.[12] In this study, we further identified that CCN1 mediates the protective role of cardiomyocyte senescence and SASP, indicating that SASP influences tissue remodeling in a context-dependent manner.[12] However, we still do not know the functional roles of the other SASP components, such as IL-1α and TNF-α. After 4 weeks of infarction, the ejection fraction was significantly decreased in the GATA4-shRNA transfected group. This decrease may result from increased "LVID" and "LV vol," which showed increased trend without statistical significance because of the inherent variation among animals. In our study, we observed that *Gata4*-shRNA reserved the post-AMI function 1 day after AMI and before CCN1 increase (Figure S5A and S5B). By contrast, when CCN1 was significantly increased 4 weeks after AMI (Figure 2D and 2H), GATA4 knockdown was detrimental to heart function. The working model is summarized in Figure 7: senescence causes senescence-related cellular dysfunction directly; senescence-related CCN1 secretion prevented pathological fibrosis to protect hearts. Specifically, there is a balance between senescence-related dysfunction and CCN1-mediated protective effects in the heart. The results from ALDH2 knockout mice also support the dual roles of cardiomyocyte senescence. In knockout mice, it was noticed that CCN1 was unaltered in the border heart tissues, and even decreased in $p16^{INK4a}$-positive cells. This observation was different from that obtained with the wild-type and caused the different outcome of GATA4 inhibition. Understanding the diverse roles and mechanisms of cardiomyocyte senescence helps develop new drugs and determine appropriate clinical strategies. Therefore, regulating the GATA4-related pathway is promising for improving cardiac remodeling in ALDH2 mutant-type people or in conditions of ALDH2 inactivation, such as nitrate tolerance and hyperglycemia.

In this study, we verified that GATA4 inhibition deteriorated the post-AMI heart function resulting from downregulated CCN1 secretion. However, whether CCN1 is a direct or indirect transcriptional target of GATA4 remains unknown, and further experimental studies are needed. In addition, it is established that senescence and SASP affect tissue and organ function in a context-dependent manner.[12,28] For example, CCN1 is essential to the proliferation of certain cell types.[29,30] By contrast, CCN1 can induce cell apoptosis and senescence during cancer development and fibrosis. In our opinion, this situation may be because of the crosstalk between CCN1 and other factors or the micro-environment, which need further study. Thus, the utility of anti-CCN1 therapy in fibrosis and cancer have to be very carefully considered. In summary, we uncovered an activated senescence phenotype in post-AMI and other heart disease models. This phenotype was observed to influence post-AMI heart remodeling via a GATA4-CCN1-fibrosis pathway.

Sources of Funding

This study was supported by the National Natural Science Foundation of China (81570401, 81571934, 81300103, 81671952), Taishan Scholar Program of Shandong Province (ts20130911), Taishan Young Scholar Program of Shandong Province, Specialized Research Fund for the Doctoral Program of Higher Education (20130131110048), Key Technology Research and Development Program of Science and Technology of Shandong Province (2014kjhm0102), Key Research and Development Program of Shandong Province (2014GSF11811, 2016GSF201235, 2016ZDJS07A14), and the Fundamental Research Funds of Shandong University (2014QLKY04).

Disclosures

None.

References

1. Singh JA, Lu X, Ibrahim S, Cram P. Trends in and disparities for acute myocardial infarction: an analysis of Medicare claims data from 1992 to 2010. *BMC Med*. 2014;12:190–202.
2. Gerczuk PZ, Kloner RA. An update on cardioprotection: a review of the latest adjunctive therapies to limit myocardial infarction size in clinical trials. *J Am Coll Cardiol*. 2012;59:969–978.
3. Dondo TB, Hall M, West RM, Jernberg T, Lindahl B, Bueno H, Danchin N, Deanfield JE, Hemingway H, Fox KAA, Timmis AD, Gale CP. Beta-blockers and mortality after acute myocardial infarction in patients without heart failure or ventricular dysfunction. *J Am Coll Cardiol*. 2017;69:2710–2720.
4. Torabi A, Cleland JG, Rigby AS, Sherwi N. Development and course of heart failure after a myocardial infarction in younger and older people. *J Geriatr Cardiol*. 2014;11:1–12.
5. Hayflick L, Moorhead PS. The serial cultivation of human diploid cell strains. *Exp Cell Res*. 1961;25:585–621.
6. Spyridopoulos I, Isner JM, Losordo DW. Oncogenic ras induces premature senescence in endothelial cells: role of p21(Cip1/Waf1). *Basic Res Cardiol*. 2002;97:117–124.
7. Meng A, Wang Y, Van Zant G, Zhou D. Ionizing radiation and busulfan induce premature senescence in murine bone marrow hematopoietic cells. *Cancer Res*. 2003;63:5414–5419.
8. Muñoz-Espín D, Cañamero M, Maraver A, Gómez-López G, Contreras J, Murillo-Cuesta S, Rodríguez-Baeza A, Varela-Nieto I, Ruberte J, Collado M, Serrano M. Programmed cell senescence during mammalian embryonic development. *Cell*. 2013;155:1104–1118.
9. Melk A. Senescence of renal cells: molecular basis and clinical implications. *Nephrol Dial Transplant*. 2003;18:2474–2478.
10. Meyer K, Hodwin B, Ramanujam D, Engelhardt S, Sarikas A. Essential role for premature senescence of myofibroblasts in myocardial fibrosis. *J Am Coll Cardiol*. 2016;67:2018–2028.
11. Tchkonia T, Zhu Y, van Deursen J, Campisi J, Kirkland JL. Cellular senescence and the senescent secretory phenotype: therapeutic opportunities. *J Clin Invest*. 2013;123:966–972.
12. Kang C, Xu Q, Martin TD, Li MZ, Demaria M, Aron L, Lu T, Yankner BA, Campisi J, Elledge SJ. The DNA damage response induces inflammation and senescence by inhibiting autophagy of GATA4. *Science*. 2015;349:aaa5612–aaa5638.
13. Jun JI, Lau LF. The matricellular protein CCN1 induces fibroblast senescence and restricts fibrosis in cutaneous wound healing. *Nat Cell Biol*. 2010;12:676–685.
14. Kim KH, Chen CC, Monzon RI, Lau LF. Matricellular protein CCN1 promotes regression of liver fibrosis through induction of cellular senescence in hepatic myofibroblasts. *Mol Cell Biol*. 2013;33:2078–2090.
15. Zhao X, Ding EY, Yu OM, Xiang SY, Tan-Sah VP, Yung BS, Hedgpeth J, Neubig RR, Lau LF, Brown JH, Miyamoto S. Induction of the matricellular protein CCN1 through RhoA and MRTF-A contributes to ischemic cardioprotection. *J Mol Cell Cardiol*. 2014;75:152–161.
16. Maejima Y, Adachi S, Ito H, Hirao K, Isobe M. Induction of premature senescence in cardiomyocytes by doxorubicin as a novel mechanism of myocardial damage. *Aging Cell*. 2008;7:125–136.
17. Niemann B, Chen Y, Teschner M, Li L, Silber RE, Rohrbach S. Obesity induces signs of premature cardiac aging in younger patients: the role of mitochondria. *J Am Coll Cardiol*. 2011;57:577–585.
18. Fountoulaki K, Dagres N, Iliodromitis EK. Cellular communications in the heart. *Card Fail Rev*. 2015;1:64–68.
19. Gao E, Lei YH, Shang X, Huang ZM, Zuo L, Boucher M, Fan Q, Chuprun JK, Ma XL, Koch WJ. A novel and efficient model of coronary artery ligation and myocardial infarction in the mouse. *Circ Res*. 2010;107:1445–1453.
20. Committee for the Update of the Guide for the Care and Use of Laboratory Animals, Institute for Laboratory Animal Research, Division on Earth and Life Studies, National Research Council of the National Academies. *Guide for the Care and Use of Laboratory Animals*. 8th ed. Washington, DC: National Academies Press; 2011.
21. Wang JL, Wang HG, Hao PP, Xue L, Wei SJ, Zhang Y, Chen YG. Inhibition of aldehyde dehydrogenase 2 by oxidative stress is associated with cardiac dysfunction in diabetic rats. *Mol Med*. 2011;17:172–179.
22. Louch WE, Sheehan KA, Wolska BM. Methods in cardiomyocyte isolation, culture, and gene transfer. *J Mol Cell Cardiol*. 2011;51:288–298.
23. Xue L, Cui SM, Cui ZQ, Yang F, Pang JJ, Xu F, Chen YG. ALDH2: a new protector against age-independent myocardial senescence. *Int J Cardiol*. 2016;210:38–40.
24. Liu BS, Wang JL, Li MH, Yuan QH, Xue MY, Xu F, Chen YG. Inhibition of ALDH2 by O-GlcNAcylation contributes to the hyperglycemic exacerbation of myocardial ischemia/reperfusion injury. *Oncotarget*. 2017;8:19413–19426.
25. Pang JJ, Wang JL, Zhang YM, Xu F, Chen YG. Targeting acetaldehyde dehydrogenase 2 (ALDH2) in heart failure-recent insights and perspectives. *Biochim Biophys Acta*. 2017;1863:1933–1941.
26. Wu B, Yu L, Wang YS, Wang HT, Li C, Yin Y, Yang JR, Wang ZF, Zheng QS, Ma H. Aldehyde dehydrogenase 2 activation in aged heart improves the autophagy by reducing the carbonyl modification on SIRT1. *Oncotarget*. 2016;7:2175–2188.
27. Muñoz-Espín D, Serrano M. Cellular senescence: from physiology to pathology. *Nat Rev Mol Cell Biol*. 2014;15:482–496.
28. Lecot P, Alimirah F, Desprez PY, Campisi J, Wiley C. Context-dependent effects of cellular senescence in cancer development. *Br J Cancer*. 2016;114:1180–1184.
29. Franzen CA, Chen CC, Todorović V, Juric V, Monzon RI, Lau LF. The matrix protein CCN1 is critical for prostate carcinoma cell proliferation and TRAIL-induced apoptosis. *Mol Cancer Res*. 2009;7:1045–1055.
30. Mo FE, Lau LF. The matricellular protein CCN1 (CYR61) is essential for cardiac development. *Circ Res*. 2006;99:961–969.

SUPPLEMENTAL MATERIAL

Table S1. The catalog number of the antibodies used in this study.

anti-p53	abcam	ab28
anti-p16INK4a	abcam	ab54210
anti-p16INK4a	abcam	ab51243
anti- p21CIP1/WAF1	abcam	ab109199
anti-GATA4	Santa-Cru	SC-1237
anti-GATA4	abcam	ab84593
anti-CCN1	abcam	ab24448
anti-γ-H2AX	abcam	ab11175
anti-γ-H2AX	CST	9718
anti-GAPDH	Proteinte	60004
anti-β-actin	Boster	BM0005
anti-IL-1α	Proteinte	16765
anti-MCP-1	abcam	ab54214
anti-TNF-α	abcam	ab8358
anti-α-actin	Proteinte	66125

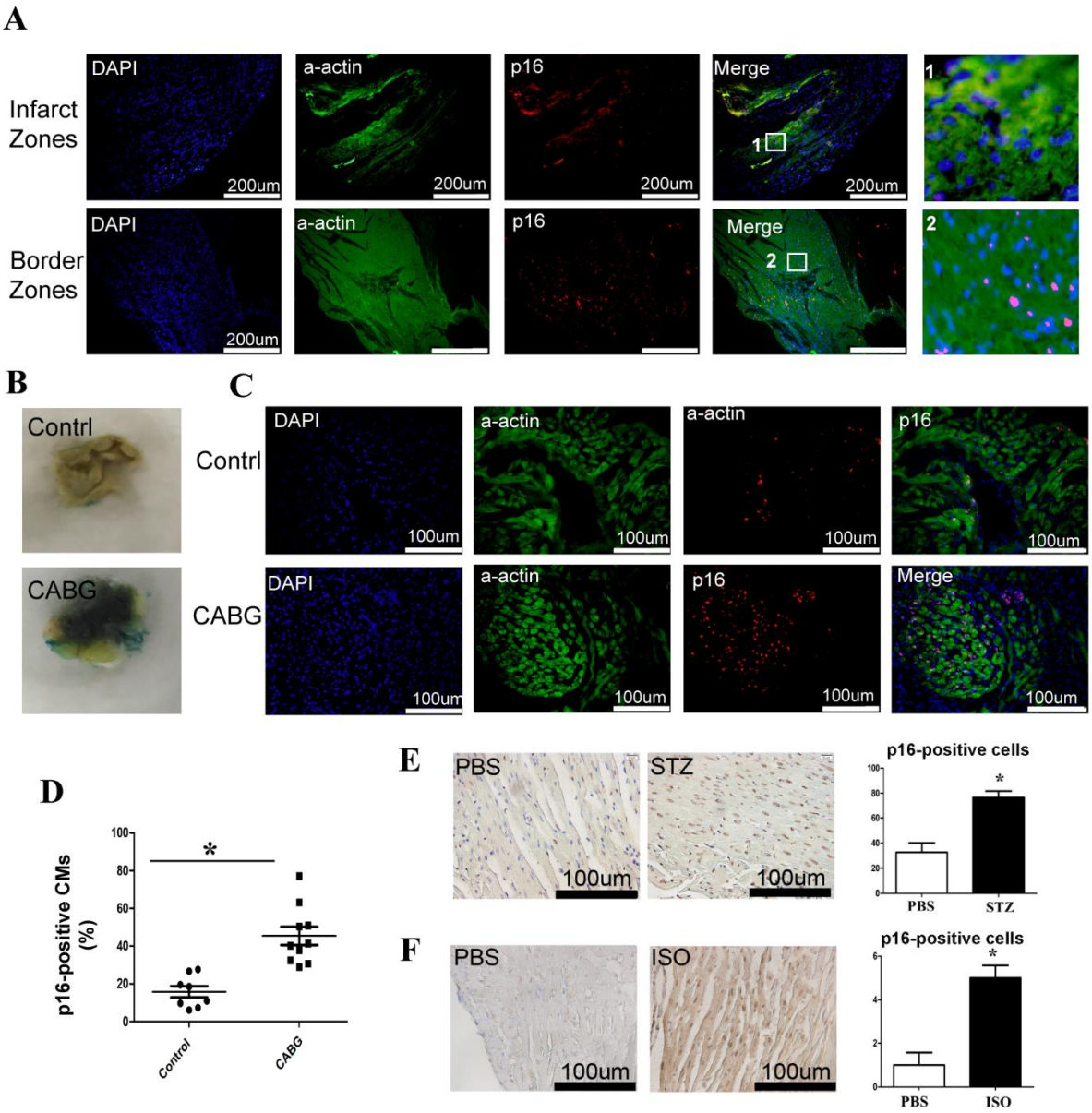

Figure S1. Senescent markers increased in several heart disease models.

A. Immunofluorescence staining images for DAPI (blue), α-actin (green), and $p16^{INK4a}$ (red) α-actin in the 4-week-postinfarction hearts.

B. SA-β-gal staining pictures in the right arterial tissues from CABG and control patients.

C. Immunofluorescence staining images for DAPI (blue), α-actin (green), and $p16^{INK4a}$ (red) in the right auricle from control and CABG patients.

D. The quantification of $p16^{INK4a}$-positive cardiomyocytes between control and CABG heart tissues.

E. Representative $p16^{INK4a}$ immunostaining pictures and quantitative analysis in the ISO-induced and PBS-treated rat hearts. *P < 0.05 vs PBS; (n≥6).

F. Representative $p16^{INK4a}$ immunostaining pictures and quantitative analysis in the ISO-induced and PBS-treated rat hearts. *P < 0.05 vs PBS; (n≥6).

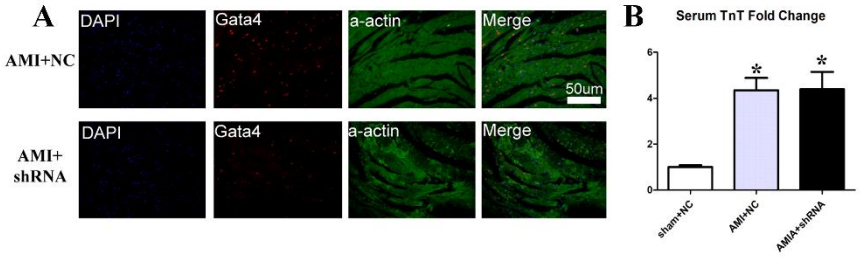

Figure S2. AAV9-*Gata4*-shRNA administration suppressed GATA4 expression after AMI.

A. Immunofluorescence staining images for DAPI (blue), Gata4(red), and α-actin (green) in the mouse hearts transfected with AAV9-*Gata4*-shRNA or negative control vectors.

B. The fold change of cardiac TnT levels in serum 24hrs post-infarct by Elisa. * P < 0.05 vs Sham+NC; (n≥6).

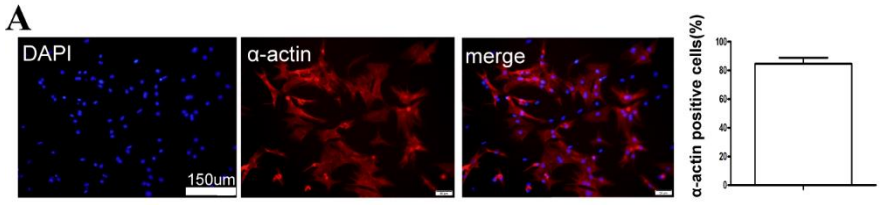

Figure S3. Cardiomyocytes were isolated from neonatal rats.

A. Representative immunofluorescence images of α-actin α-actin in the isolated NRCMs.

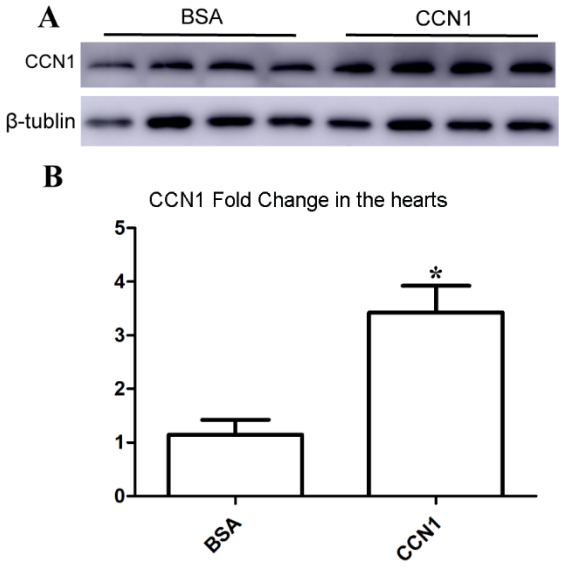

Figure S4. Exogenous CCN1 protein administration significantly increased CCN1 levels in the hearts.

A. Western blotting was utilized to examine the CCN1 protein change in the heart after 24 hours of CCN1 injection.

B. Quantitative analysis of the CCN1 increase in the heart after 24 hours of CCN1 injection. * $P < 0.05$(n=4).

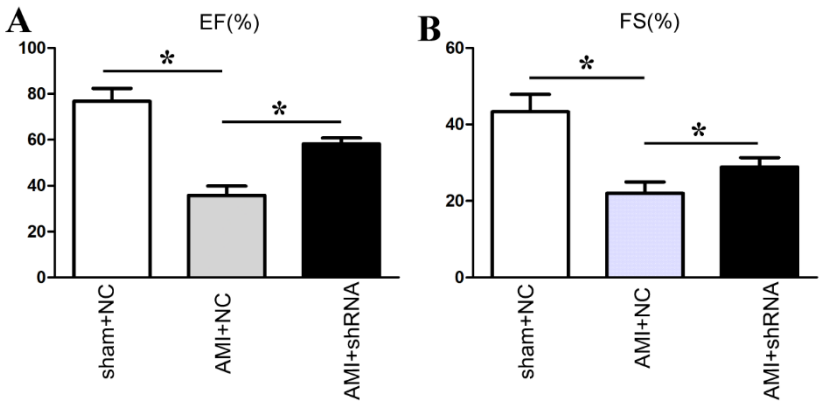

Figure S5. AAV9-*Gata4*-shRNA administration improved the heart function one day after infarction.

A. Echocardiography showed that the effects of *Gata4*-shRNA transfected on the EF(A) and FS(B) 1 day after AMI. *: $P < 0.05$ (n≥6).